Intramolecular Hydrogen Bonding in Derivatives of β-Alanine and γ-Amino Butyric Acid: Model Studies for the Folding of Unnatural Polypeptide Backbones

Gregory P. Dado and Samuel H. Gellman*

Contribution from the S. M. McElvain Laboratory of Organic Chemistry, Department of Chemistry, University of Wisconsin, 1101 University Avenue, Madison, Wisconsin 53706

Received August 19, 1993®

Abstract: We have examined the intramolecular hydrogen bonding behavior of simple β- and γ-amino acid derivatives as a prelude to efforts to design unnatural polyamides that will adopt compact and specific folding patterns analogous to those of α-amino acid polymers (proteins). We postulate that the desired folding behavior will be most likely if intramolecular hydrogen bonds are unfavorable between nearest neighbor amide groups on the polymer backbone. Previous work from other laboratories and our own has shown that this criterion applies to α-amino acid polymers. Variable-temperature FT-IR data reported here for β-alanine derivatives in methylene chloride indicate that nearest neighbor hydrogen bonding is unfavorable for this type of residue as well. FT-IR and NMR data for γ-amino butyric acid derivatives, however, show that nearest neighbor hydrogen bonding is favorable. For two of the diamides discussed here, thermodynamic parameters have been determined for hydrogen-bond-mediated folding via variable-temperature FT-IR measurements. These $\Delta H°$ and $\Delta S°$ values should provide useful benchmarks for molecular mechanics programs.

Polymers of α-amino acids have intrinsically flexible backbones, yet many proteins adopt very compact conformations that are thermodynamically and kinetically stable under physiological conditions.[1,2] The integrity of protein-folding patterns is crucial to proper function, because groups that are remotely spaced along the peptide's linear sequence must often be precisely positioned near one another for activity.[2,3] The remarkable range of functions performed by natural proteins leads the chemist to wonder whether other types of polymers might also fold to specific, compact conformations, thereby generating "active sites".

The design of unnatural polymers that adopt compact and specific folding patterns is a challenge because, despite decades of intensive study, the origins of protein conformational stability are still not completely clear.[4] It seems generally agreed that any particular protein's tertiary structure reflects the balance achieved among a large number of energetically weak nonbonded interactions; however, it is still impossible to predict detailed folding patterns based simply on a knowledge of amino acid sequence.

In spite of the many lingering mysteries in the realm of protein folding, it is possible to define general features that are crucial to the ability of α-amino acid polymers to adopt compact conformations that display long-range order. One such feature seems to be the capacity for some type of attractive interaction, in which interaction energy depends upon geometry, between different sites on the polymer backbone. In proteins, hydrogen bonds are the most obvious interactions of this type. Because hydrogen-bond energy depends upon interatomic distances and angles,[5] intramolecular hydrogen bonds can serve a structure-specifying role in folded proteins, helping to distinguish energetically among alternative compact conformations. (Another possible function of intramolecular hydrogen bonds, stabilization of the folded state of proteins relative to unfolded states,[6] is contested; some workers argue that this contribution will be small, since intramolecular hydrogen bonds lost upon unfolding are replaced by hydrogen bonds to the solvent.[4,7])

Chart 1. The Two Common Short-Range Hydrogen Bonds Involving Backbone Amide Groups in α-Amino Acid Polymers

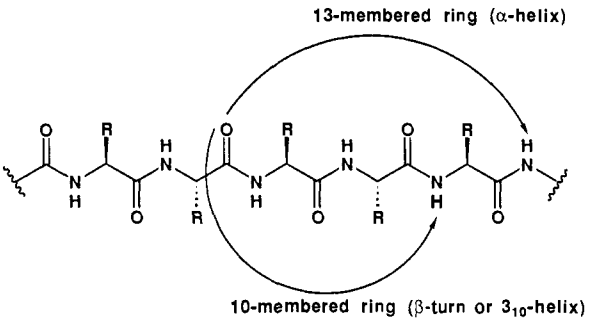

Two aspects of the covalent structure of α-amino acid polymers seem to be essential in the context of the structure-specifying role of intramolecular hydrogen bonds. First, the repeating backbone structure contains both hydrogen-bond donors (amide N–H) and hydrogen-bond acceptors (amide C=O). Second, *the covalent spacing of these repeating hydrogen-bonding groups is such that interactions between nearest neighbor amide groups are not favorable* (*vide infra*). In contrast, hydrogen bonds between more covalently distant backbone amide groups are favorable, at least in some cases (Chart 1). If one intervening amide group is skipped, a 10-membered-ring hydrogen bond can be formed, which is commonly observed in β-turns and the 3_{10}-helix. If two intervening amide groups are skipped, a 13-membered-ring hydrogen bond can be formed, which is characteristic of the α-helix. Both of these common hydrogen-bonded ring sizes involve a C=O- -H—N alignment that runs in the N- to C-terminal direction. Hydrogen bonds with the alternative C- to N-terminal C=O- -H—N alignment are also possible with one or two

* Abstract published in *Advance ACS Abstracts*, January 1, 1994.

(1) Richardson, J. S. *Adv. Protein Chem.* **1981**, *34*, 167.

(2) Creighton, T. E. *Proteins: Structures and Molecular Principles*, 2nd ed.; Freeman: New York, 1993.

(3) Fersht, A. *Enzyme Structure and Mechanism*, 2nd ed.; Freeman: New York, 1985.

(4) Dill, K. A. *Biochemistry* **1990**, *29*, 7133.

(5) For leading references, see: (a) Luck, W. A. P. In *The Hydrogen Bond*; Schuster, P., Ed.; North Holland Publishing Co.: Amsterdam, The Netherlands, 1976; Vol. II, p 577. (b) Allen, L. C.; Kerns, R. C. *J. Am. Chem. Soc.* **1978**, *100*, 6587. (c) Peters, D.; Peters, J. *J. Mol. Struct.* **1980**, *68*, 255. (d) Vedani, A.; Dunitz, J. D. *J. Am. Chem. Soc.* **1985**, *107*, 7653. (e) Mitchell, J. B. O.; Price, S. L. *Chem. Phys. Lett.* **1989**, *154*, 267. (f) Guo, H.; Karplus, M. *J. Phys. Chem.* **1992**, *96*, 7273.

(6) Shirley, B. A.; Stanssens, P.; Hahn, U.; Pace, C. N. *Biochemistry* **1992**, *31*, 725.

(7) Klotz, I. M.; Franzen, J. S. *J. Am. Chem. Soc.* **1962**, *84*, 3461.

0002-7863/94/1516-1054$04.50/0

Chart 2. The Two Possible Hydrogen Bonds between Nearest Neighbor Amide Groups in α-Amino Acid Polymers

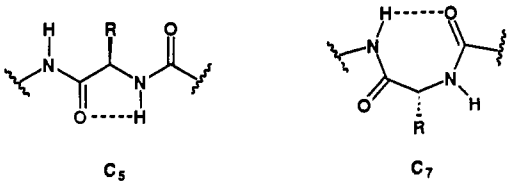

C_5 C_7

intervening amides (involving 8- and 11-membered rings, respectively), but these hydrogen-bonding arrangements are rare in proteins.[8]

Several lines of evidence indicate that formation of hydrogen bonds between nearest neighbor amide groups in an α-amino acid polymer backbone does not provide a substantial energetic benefit. Two such hydrogen bonds are formally possible, involving five- and seven-membered-ring interactions (designated C_5 and C_7, respectively; Chart 2).[9,10] It is generally believed that amide-to-amide hydrogen bonds are strongest when the N–H- -O angle is linear or nearly so;[5] the C_5-type hydrogen bond is therefore not expected to result in a strong attraction because this interaction necessarily has a dramatic deviation from linearity (N–H- -O angle $\leq 100°$).[5c] The C_7-type hydrogen bond is very rare among the folded proteins that have been characterized crystallographically,[8,11] which suggests that this interaction is not important in stabilizing protein folding patterns. A number of laboratories have examined the adoption of the C_7 folding pattern by simple model peptides in solution.[9,10,12] Careful IR studies by Maxfield et al. have shown that single-residue peptides **1a–c** in $CHCl_3$

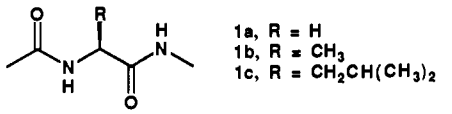

1a, R = H
1b, R = CH_3
1c, R = $CH_2CH(CH_3)_2$

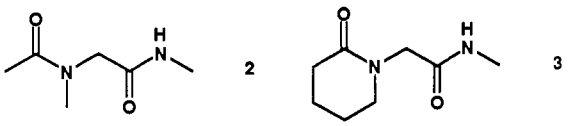

2 **3**

solution at room temperature experience no C_7-type hydrogen bonding;[13] we have made similar observations for alanine derivative **1b** in CH_2Cl_2.[14] In contrast, analogous single-residue peptides constructed from *N*-alkyl-α-amino acids (e.g., **2**) show a significant population of the C_7 folding pattern in chlorocarbon solvents.[15] Evaluating the extent of the C_7 population in such cases is difficult, however, because of *cis–trans* isomerism about the tertiary amide C–N bond (only the *trans* configuration is populated for most secondary amides). To overcome this ambiguity, we recently characterized the folding properties of **3**, the lactam ring of which precludes an unnatural configuration about the tertiary amide C–N bond.[16] Variable-temperature IR data indicate that the intramolecularly hydrogen bonded (C_7) and non-hydrogen-bonded states of **3** are of nearly identical enthalpy in CH_2Cl_2. Thus, even in a solvent that is incapable of forming strong hydrogen bonds, the enthalpic gain from formation of the seven-membered-ring C=O- -H—N hydrogen bond is counterbalanced by unfavorable interactions that develop as the molecule folds back upon itself. This counterbalancing results at least in part from the fact that the N—H- -O=C hydrogen bond must deviate substantially from linearity, because of the seven-membered ring constraint.

In contemplating unnatural polymer backbones that might be conducive to the adoption of compact and specific folded conformations, we were drawn to structures derived from β- and γ-amino acids, since such "β-peptides" and "γ-peptides" would retain the secondary amide groups that allow hydrogen-bond donation and acceptance in "α-peptides" (i.e., naturally occurring peptides and proteins).[17,18] As a prelude to examining the folding of oligomeric β-peptides and γ-peptides, however, it seemed necessary to determine whether conformations containing intramolecular hydrogen bonds between nearest neighbor amide groups would be favorable in such structures. As discussed above, we believe that a strong tendency for such nearest neighbor interactions would work against the adoption of folding patterns that display long-range order. We report here on the folding behavior of β-alanine and γ-amino butyric acid derivatives **4–9** in methylene chloride. In each of diamides **4–7**, only a single intramolecular amide-to-amide hydrogen bond is possible; in **8** and **9**, two alternative hydrogen-bonding patterns can potentially compete with one another.

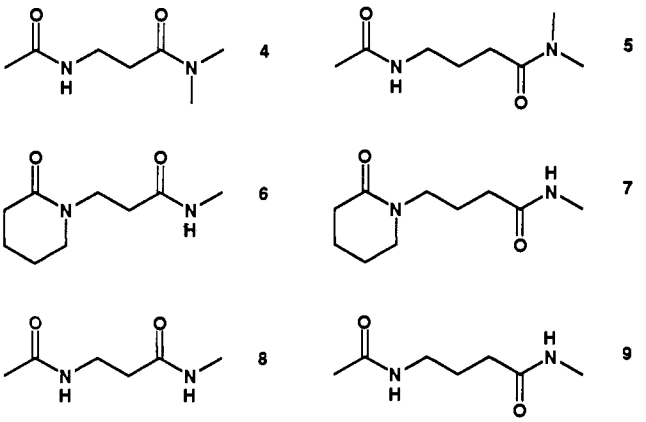

4 **5** **6** **7** **8** **9**

Marraud and Neel have previously examined β-alanine derivative **8** in CCl_4 solution at room temperature by IR.[19] As we have, these workers chose **4** as their reference compound for six-membered-ring hydrogen-bond formation, but they chose **10** as their reference for eight-membered-ring hydrogen bonding. It was necessary to reinvestigate **4** and **8** for several reasons: (i) we wanted a direct comparison of analogous β-alanine and γ-amino butyric acid derivatives; (ii) we wanted to carry out low-temperature studies (in pursuit of thermodynamic parameters), which required a non-hydrogen-bonding solvent more polar than CCl_4, since small amides have a strong tendency to aggregate in CCl_4;[13] and (iii) we wanted to examine lactam **6** instead of **10**, because there is no structural ambiguity arising from slow rotameric interconversion about the tertiary amide C–N bond of **6**.

(8) Baker, E. N.; Hubbard, R. E. *Prog. Mol. Biol. Biophys.* **1984**, *44*, 97.
(9) Tsuboi, M.; Shimanouchi, T.; Mizushima, S. *J. Am. Chem. Soc.* **1959**, *81*, 1406.
(10) (a) Avignon, M.; Huong, P. V.; Lascombe, J.; Marraud, M.; Neel, J. *Biopolymers* **1969**, *8*, 69. (b) Neel, J. *Pure Appl. Chem.* **1972**, *31*, 201.
(11) Milner-White, E. J.; Ross, B. M.; Ismail, R.; Belhadj-Mostefa, K.; Poet, R. *J. Mol. Biol.* **1988**, *204*, 777.
(12) For leading references, see: Madison, V.; Kopple, K. D. *J. Am. Chem. Soc.* **1980**, *102*, 4855.
(13) Maxfield, F. R.; Leach, S. J.; Stimson, E. R.; Powers, S. P.; Scheraga, H. A. *Biopolymers* **1979**, *18*, 2507.
(14) Liang, G.-B. Ph.D. Thesis, University of Wisconsin—Madison, 1992.
(15) Mizushima, S.; Shimanogouchi, T.; Tsuboi, M.; Arakawa, T. *J. Am. Chem. Soc.* **1957**, *79*, 5357.
(16) Dado, G. P.; Gellman, S. H. *J. Am. Chem. Soc.* **1992**, *114*, 3138.
(17) We have previously examined the folding behavior of a number of unnatural oligoamide structures: (a) Gellman, S. H.; Adams, B. R.; Dado, G. P. *J. Am. Chem. Soc.* **1990**, *112*, 460. (b) Dado, G. P.; Desper, J. M.; Holmgren, S. K.; Rito, C. J.; Gellman, S. H. *J. Am. Chem. Soc.* **1992**, *114*, 4834. (c) Liang, G.-B.; Desper, J. M.; Gellman, S. H. *J. Am. Chem. Soc.* **1993**, *115*, 925. (d) Dado, G. P.; Gellman, S. H. *J. Am. Chem. Soc.* **1993**, *115*, 4228.
(18) Recent studies of folding in unnatural urea and amide oligomers: (a) Nowick, J. S.; Powell, N. A.; Martinez, E. J.; Smith, E. M.; Noronha, G. *J. Org. Chem.* **1992**, *57*, 3763. (b) Hagihara, M.; Anthony, N. J.; Stout, T. J.; Clardy, J.; Schreiber, S. L. *J. Am. Chem. Soc.* **1992**, *114*, 6568.
(19) Marraud, M.; Neel, J. *J. Polym. Sci.* **1975**, 271.

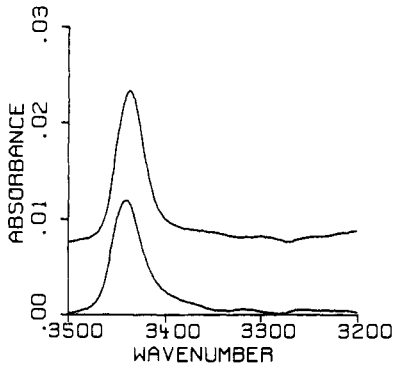

Figure 1. N–H stretch region FT-IR data for 1 mM **4** in CH_2Cl_2 at 293 K (bottom; maximum at 3440 cm^{-1}) and 205 K (top; maximum at 3436 cm^{-1}), after subtraction of the spectrum of pure CH_2Cl_2 at the same temperature.

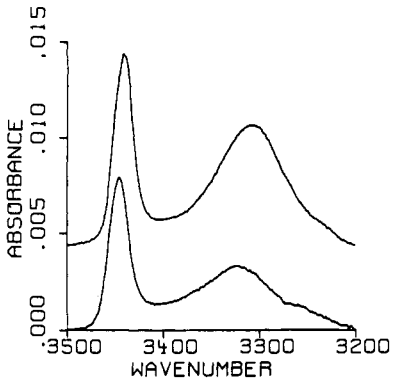

Figure 2. N–H stretch region FT-IR data for 1 mM **5** in CH_2Cl_2 at 294 K (bottom; maxima at 3446 and 3323 cm^{-1}) and 205 K (top; maximum at 3441 and 3307 cm^{-1}), after subtraction of the spectrum of pure CH_2Cl_2 at the same temperature.

Scheme 1. Synthesis of Lactams 6 and 7[a]

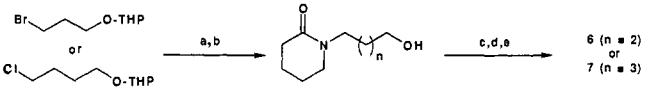

[THP = tetrahydropyran protecting group]

[a] Key: (a) valerolactam, KOH, nBu_4NBr, THF; (b) Amberlyst-15, MeOH; (c) oxalyl chloride, DMSO, CH_2Cl_2, –60 °C; Et_3N; (d) $AgNO_3$, NaOH, H_2O, 0 °C; (e) DCC, HOSu, THF; CH_3NH_2.

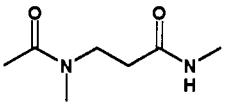

10

Results

Diamides **4**, **5**, **8**, and **9** were prepared from β-alanine or γ-amino butyric acid using standard synthetic methods, as described in the Experimental Section. The syntheses of lactam-based amides **6** and **7** is outlined in Scheme 1; details may be found in the Experimental Section.

Figure 1 shows N–H stretch region IR data for 1 mM **4** in CH_2Cl_2 at 293 and 205 K. Only a single N–H stretch band is observed in each case, at 3440 and 3436 cm^{-1}. These band positions indicate a non-hydrogen-bonded N–H;[20] thus, the six-membered-ring hydrogen bond available to β-alanine derivative **4** does not form. These IR data also show that no hydrogen-bond-mediated aggregation of **4** occurs under these conditions. Figure 2 shows analogous IR data for 1 mM **5** in CH_2Cl_2. In this case, two N–H stretch bands are observed at each temperature; band positions at 294 K are 3446 and 3323 cm^{-1}. The higher energy band arises from a non-hydrogen-bonded N–H, and the lower energy band, from an intramolecularly hydrogen bonded N–H. The relative band proportions indicate qualitatively that the seven-membered-ring hydrogen bond available to γ-amino butyric acid derivative **5** is formed to a considerable extent.

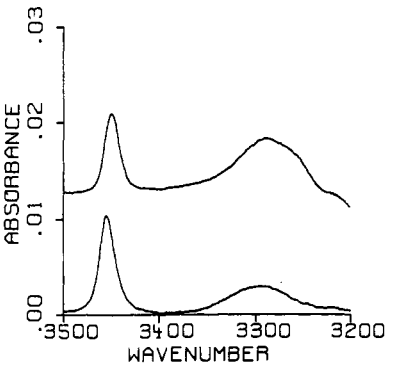

Figure 3. N–H stretch region FT-IR data for 1 mM **6** in CH_2Cl_2 at 293 K (bottom; maxima at 3455 and 3295 cm^{-1}) and 204 K (top; maxima at 3450 and 3288 cm^{-1}), after subtraction of the spectrum of pure CH_2Cl_2 at the same temperature.

Figure 3 shows N–H stretch region IR data for lactam-containing β-alanine derivative **6**, 1 mM in CH_2Cl_2. At 293 K, the broad band at 3295 cm^{-1} indicates formation of the eight-membered-ring hydrogen bond, and it is clear from the change in band proportions at 204 K that the extent of intramolecular hydrogen bonding increases at lower temperature. We have previously shown that variable-temperature IR data of this type may be used to derive $\Delta H°$ and $\Delta S°$ values for hydrogen-bond-mediated folding in small amides.[17c,d,21,22] Such systems are analyzed in terms of an equilibrium between two states, non-hydrogen bonded and intramolecularly hydrogen bonded (eq 1);

$$\text{non-hydrogen bonded} \overset{K_{eq}}{\rightleftarrows} \text{intramolecularly hydrogen bonded} \quad (1)$$

$$\ln K_{eq} = -\Delta H°/RT + \Delta S°/R \quad (2)$$

changes in the equilibrium constant (K_{eq}) as a function of temperature can be used to derive $\Delta H°$ and $\Delta S°$ for the folding process via the van't Hoff equation (eq 2). IR data like those in Figure 3 can be used to determine the concentration of the non-hydrogen-bonded state directly, because model compounds like *N*-methylacetamide (NMA), which experience no hydrogen bonding in a 1 mM solution at any temperature in liquid CH_2Cl_2, allow one to determine the temperature-dependent integrated extinction coefficient for a representative non-hydrogen-bonded N–H stretch. In contrast, the concentration of the hydrogen-bonded state of **6** cannot be determined directly, because no fully hydrogen bonded model compound is available. Since, however, we know the total amide concentration, we can assume that the hydrogen-bonded state corresponds to that portion of the total concentration not accounted for by the non-hydrogen-bonded state. The van't Hoff plot for diamide **6** is shown in Figure 4. This analysis indicates that the eight-membered-ring hydrogen-bonded state is enthalpically favored by 1.4 kcal/mol but entropically disfavored by 5.8 e.u. relative to the non-hydrogen-bonded state (on the basis of our previous IR-based analyses of this type,[17c,d,21,22] we estimate the error in these values to be ca. ±0.2 kcal/mol and ±1 e.u.).[23]

Figure 5 shows the N–H stretch region IR data for lactam-containing γ-amino butyric acid derivative **7**. The presence of

(20) We use the term "non-hydrogen bonded" to signify the absence of strong N—H- -O=C interaction in methylene chloride solution. Such amides are presumably involved in weakly attractive interactions with the solvent.

(21) Gellman, S. H.; Dado, G. P.; Liang, G.-B.; Adams, B. R. *J. Am. Chem. Soc.* **1991**, *113*, 1164.

(22) Gallo, E. A.; Gellman, S. H. *J. Am. Chem. Soc.* **1993**, *115*, 9774.

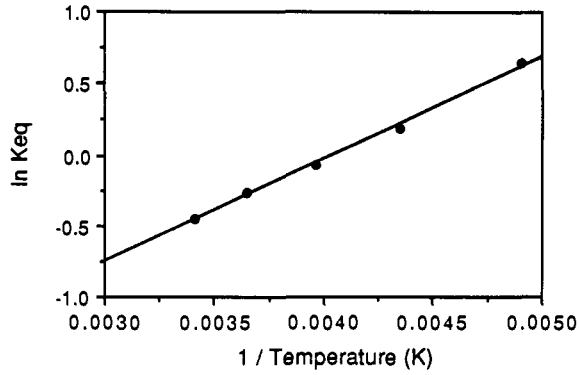

Figure 4. van't Hoff plot constructed from variable-temperature (204–293 K) N–H stretch region IR data for 1 mM **6** in CH_2Cl_2, based on a two-state conformational model, non-hydrogen bonded vs intramolecularly hydrogen bonded (eq 1). The line represents the best fit to eq 2, with $\Delta H°$ = –1.4 kcal/mol and $\Delta S°$ = –5.8 e.u. (correlation coefficient = 0.997).

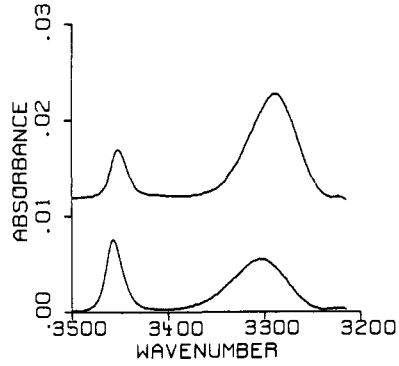

Figure 5. N–H stretch region FT-IR data for 1 mM **7** in CH_2Cl_2 at 293 K (bottom; maxima at 3457 and 3303 cm^{-1}) and 204 K (top; maxima at 3451 and 3288 cm^{-1}), after subtraction of the spectrum of pure CH_2Cl_2 at the same temperature.

two N–H stretch bands indicates that both the nine-membered-ring hydrogen-bonded and non-hydrogen-bonded states are populated; the intramolecularly hydrogen bonded state is dominant at the lower temperature. Quantitative analysis was carried out using the temperature-dependent integrated extinction coefficient for the non-hydrogen-bonded N–H stretch band of NMA to determine the concentration of the non-hydrogen-bonded state of **7**, as described above. The van't Hoff plot is shown in Figure 6. This analysis indicates that the nine-membered-ring hydrogen-bonded state is enthalpically favored by 1.5 kcal/mol but entropically disfavored by 4.7 e.u. relative to the non-hydrogen-bonded state.[23]

The IR-based thermodynamic analyses of intramolecular hydrogen bond formation in **6** and **7** depend upon the assumption that no intermolecular hydrogen bonding occurs throughout the temperature range examined. Figure 7 shows data that support this assumption. IR spectra were obtained at 203 K for 2.5 and 0.25 mM solutions of **6** and **7** in CH_2Cl_2. For each diamide, the 0.25 mM spectrum was multiplied by ten and subtracted from the 2.5 mM spectrum. The resulting difference spectra show no

(23) We have previously reported (refs 17c,d and 21) good agreement between NMR-based and IR-based van't Hoff analysis of hydrogen-bond-mediated folding in small amides. In addition to the IR-based analyses of lactams **6** and **7**, we also carried out NMR-based analyses (for details, see: Dado, G. P. Ph.D. Thesis, University of Wisconsin—Madison, 1993). For **6** in CD_2Cl_2, the NMR-based analysis indicated the intramolecularly hydrogen bonded form to be enthalpically favored by 1.1 kcal/mol but entropically disfavored by 4.9 e.u. relative to the non-hydrogen-bonded form. For **7**, the NMR-based analysis indicated the intramolecularly hydrogen bonded form to be enthalpically favored by 1.2 kcal/mol but entropically disfavored by 4.3 e.u. These $\Delta H°$ and $\Delta S°$ values are in reasonably good agreement with the IR-based values reported in the text, although the agreement for the $\Delta H°$ values is poorer than in previously reported cases.

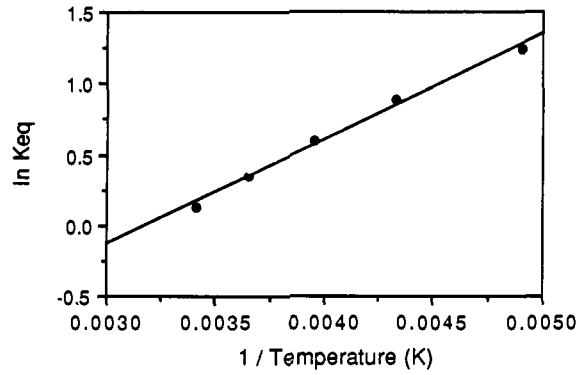

Figure 6. van't Hoff plot constructed from variable-temperature (204–293 K) N–H stretch region IR data for 1 mM **7** in CH_2Cl_2, based on a two-state conformational model, non-hydrogen bonded vs intramolecularly hydrogen bonded (eq 1). The line represents the best fit to eq 2, with $\Delta H°$ = –1.5 kcal/mol and $\Delta S°$ = –4.7 e.u. (correlation coefficient = 0.993).

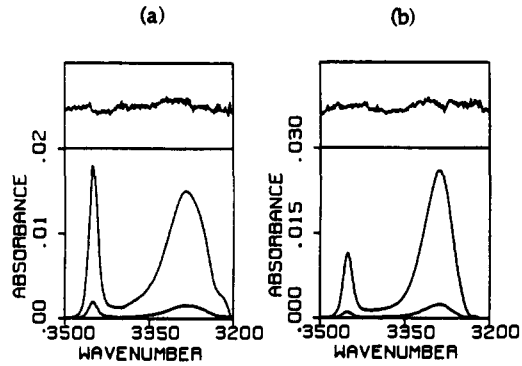

Figure 7. N–H stretch region FT-IR data for (a) 0.25 and 2.5 mM **6** and (b) 0.25 and 2.5 mM **7** in CH_2Cl_2 at 203 K, after subtraction of the spectrum of pure CH_2Cl_2 at that temperature. The upper boxes show difference spectra obtained by subtracting ten times the 0.25 mM spectrum from the 2.5 mM spectrum.

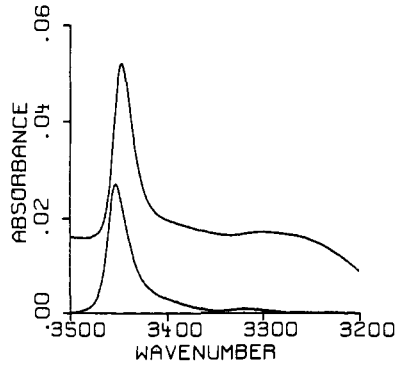

Figure 8. N–H stretch region FT-IR data for 1 mM **8** in CH_2Cl_2 at 294 K (bottom; maximum at 3453 cm^{-1}) and 204 K (top; maximum at 3447 cm^{-1}), after subtraction of the spectrum of pure CH_2Cl_2 at the same temperature.

significant residual absorption, suggesting that there is no significant intermolecular hydrogen bonding under these conditions.

Figure 8 shows N–H stretch region IR data for β-alanine derivative **8**. There is no significant absorbance in the region below 3400 cm^{-1}, indicating that no intramolecular (or intermolecular) hydrogen bonding occurs between 294 and 204 K in a 1 mM CH_2Cl_2 solution. Figure 9 shows analogous IR data for γ-amino butyric acid derivative **9**. In this case, both non-hydrogen-bonded and hydrogen-bonded N–H stretch bands are observed at the high and low temperatures. Two hydrogen-bonded rings are possible for diamide **9**, involving a seven- or a nine-membered ring. Since we cannot resolve the non-hydrogen-

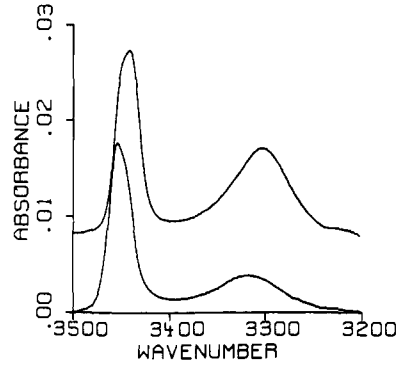

Figure 9. N–H stretch region FT-IR data for 1 mM **9** in CH_2Cl_2 at 294 K (bottom; maxima at 3454 and 3316 cm^{-1}) and 205 K (top; maxima at 3442 and 3303 cm^{-1}), after subtraction of the spectrum of pure CH_2Cl_2 at the same temperature.

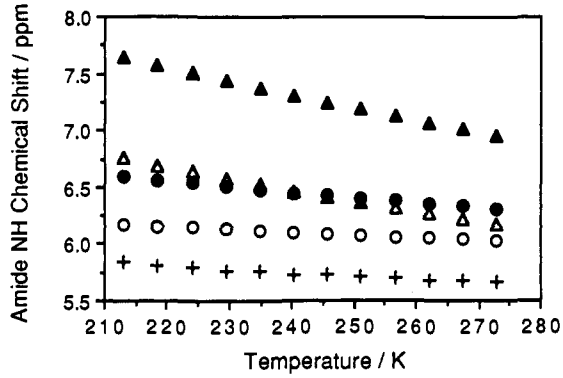

Figure 10. Amide proton NMR chemical shifts of 1 mM amide samples in CD_2Cl_2 as a function of temperature, 213–273 K: diamide **7** (▲, $\Delta\delta NH/\Delta T$ = –11.3 ppb/K), diamide **5** (●, $\Delta\delta NH/\Delta T$ = –4.8 ppb/K), C-terminal NH of diamide **9** (△, $\Delta\delta NH/\Delta T$ = –9.8 ppb/K), N-terminal NH of diamide **9** (○, $\Delta\delta NH/\Delta T$ = –2.5 ppb/K), C-terminal amide proton of diamide **8** (+, $\Delta\delta NH/\Delta T$ = –2.9 ppb/K).

bonded N–H stretch bands of the two different secondary amide groups, or the hydrogen-bonded N–H stretch bands for these groups, we cannot determine the relative extents of seven- and nine-membered-ring formation from the IR data.

We analyzed the behavior of **9** by variable-temperature ^1H NMR in CD_2Cl_2 in order to gain further insight on this molecule's folding behavior. An amide proton's chemical shift is very sensitive to that proton's hydrogen-bonded status. The utility of NMR measurements for the study of hydrogen bonding is limited, however, by two factors: (i) sources of magnetic anisotropy other than hydrogen-bond formation can influence an amide proton's chemical shift; and (ii) equilibration between hydrogen-bonded and non-hydrogen-bonded states is usually fast on the NMR time scale, which means that observed chemical shifts are weighted averages of the chemical shifts of the contributing states. (In contrast, hydrogen-bonding equilibria are slow on the IR time scale, giving rise to discrete N–H stretch bands for hydrogen-bonded and non-hydrogen-bonded states of a given secondary amide group. IR has the disadvantage, relative to NMR, of signal overlap when more than one N–H group is present, as seen with **9**.) For relatively simple amides, including small peptides, we have shown that variable-temperature ^1H NMR data obtained in nonpolar solvents (specifically, the temperature dependences of amide proton chemical shifts, $\Delta\delta NH/\Delta T$) can provide qualitative, and sometimes quantitative, information on the thermodynamic relationships among alternative folding patterns, if appropriate reference molecules are available.[17c,d,21,24]

Figure 10 shows $\Delta\delta NH/\Delta T$ data obtained for 1 mM samples of **9** and several reference compounds, **5**, **7**, and **8** (C-terminal amide proton only), in CD_2Cl_2. Variable-temperature IR data for diamide **8** (Figure 8) show that there is no significant hydrogen bonding in a 1 mM CH_2Cl_2 solution throughout the temperature range covered. Therefore, the $\Delta\delta NH/\Delta T$ signature for the C-terminal amide proton of **8** represents the behavior of an *N*-methyl amide proton in the non-hydrogen-bonded state. This resonance appears in the range 5.8–6.2 ppm, and the temperature dependence is relatively small (–2.9 ppb/K); this behavior is consistent with that previously observed for completely non-hydrogen-bonded amide protons in CD_2Cl_2.[21] Diamides **5** and **7** can each experience only one type of hydrogen bond, and the variable-temperature IR data for these diamides (Figures 2 and 5, respectively) show that in both cases the extent of intramolecular hydrogen bonding increases as the temperature is lowered. The $\Delta\delta NH/\Delta T$ signatures of the amide protons of **5** and **7** show the features expected in light of the IR results: the amide resonances of **5** and **7** are consistently downfield of the completely non-hydrogen-bonded amide proton of **8**, and both temperature dependences are larger than that of the completely non-hydrogen-bonded amide proton. The relatively large temperature dependences of these amide protons' chemical shifts reflect the increased population of hydrogen-bonded states at lower temperatures.[17c,d,21,24]

The $\Delta\delta NH/\Delta T$ signatures of **5** and **7** allow us to interpret qualitatively the hydrogen-bonding behavior of **9**. Since at all temperatures the C-terminal amide proton of **9** is upfield of the amide proton of **7**, we conclude that there is less nine-membered-ring hydrogen bonding in **9** than in **7**. Similarly, since the N-terminal amide proton of **9** is consistently upfield of the amide proton of **5**, there must be less seven-membered-ring hydrogen bonding in **9** than in **5**. The two hydrogen-bonded rings available to **9** are mutually exclusive, and the comparisons with **5** and **7** suggest that the competition between these alternative folding patterns in **9** diminishes the population of each hydrogen-bonded ring relative to situations in which only one hydrogen-bonding pattern is available. (As discussed below, other factors also affect the different extents of nine-membered-ring hydrogen-bond formation in **7** and **9**.)

The C-terminal amide proton of **9** shows a larger temperature dependence than the N-terminal proton of **9**, which indicates that formation of the nine-membered hydrogen-bonded ring is enthalpically more favorable than formation of the seven-membered hydrogen-bonded ring.[17c,d,21] This enthalpic advantage of a larger over a smaller hydrogen-bonded ring is similar to behavior we have previously observed for *N*-malonylglycine derivatives[17] and for Pro-X dipeptides[24] in organic solvents. As in those previous cases, we suspect that the larger ring available to **9** is enthalpically superior at least in part because the larger ring allows a more optimal hydrogen-bond geometry: the N–H- -O angle can be linear in the nine-membered ring, but not in the seven-membered ring.

Discussion

Nearest Neighbor Interactions in β- and γ-Peptides. Our data for diamides **4** and **8** suggest that polymers composed of β-amino acids may adopt compact and specific folding patterns, because nearest neighbor hydrogen bond formation is not a favorable process. The fact that we can detect no intramolecular hydrogen bonding for **8** between 204 and 294 K suggests that neither the six- nor the eight-membered-ring hydrogen-bonded state is particularly favorable. These results for **4** and **8** are consistent with the earlier findings of Marraud and Neel, who detected relatively little C=O- -H—N hydrogen bonding in **8** and none in **4** in CCl_4 solution at room temperature.[19] Our data for **5**, **7**, and **9** suggest that polymers composed of γ-amino acids may be less likely to adopt compact and specific folding patterns, because both types of hydrogen bonds between nearest neighbor amide

(24) Liang, G.-B.; Rito, C. J.; Gellman, S. H. *J. Am. Chem. Soc.* **1992**, *114*, 4440.

groups are favorable in this case. If nearest neighbor hydrogen bonds dominated γ-amino acid-based polymers, then the backbone amide groups would not be available for longer range hydrogen bonds of the type that appear to confer conformational specificity in folded proteins. (Of course, the hydrophobic effect might induce compact conformations for larger β- or γ-peptides in aqueous solution, but it is not clear that hydrophobic clustering among nonpolar moieties is as effective as hydrogen bonding at specifying among alternative compact conformations.)

There is an interesting contrast in behavior between **6** and **8**. We cannot detect eight-membered-ring hydrogen bonding in **8**, but the apparently analogous eight-membered-ring hydrogen bond of **6** is highly populated. (An analogous contrast may be found in comparing the lack of C_7-type hydrogen bonding in **1a** with the presence of such hydrogen bonding in **2** and **3**.) The lack of eight-membered-ring hydrogen bonding in **8** clearly does not result from competition with the alternative six-membered ring, which is not populated for **4** (i.e., when there is no other choice). Instead, the difference between the eight-membered-ring hydrogen-bonded states of **6** and **8** appears to result from the fact that the hydrogen-bond accepting amide is tertiary in the former and secondary in the latter.

There are two possible reasons for the tertiary amide group's greater tendency to engage in the eight-membered-ring intramolecular hydrogen bond. First, tertiary amides are slightly stronger hydrogen-bond acceptors than secondary amides: the hydrogen-bond enthalpy between *p*-fluorophenol and *N*-methylformamide is −6.4 kcal/mol, while the value for *N*,*N*-dimethylformamide is −7.0 kcal/mol.[25] Second, the tertiary amide nitrogen in the chain linking the hydrogen-bond donor and acceptor sites leads to a conformational restriction that is not present when a secondary amide nitrogen occupies the analogous position. This conformational restriction is analogous to $A^{1,3}$-strain in highly substituted olefins.[26] As indicated schematically below, in **8**, the C′N–$C_\beta C_\alpha$

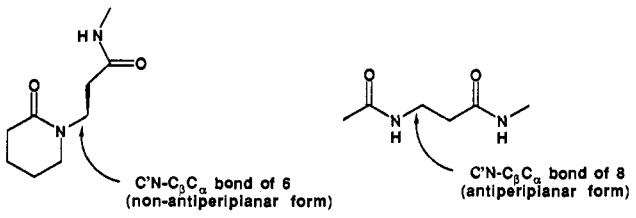

torsional unit (where C′ = acetyl group carbonyl carbon, C_β = β-carbon of the β-alanine residue, and C_α = α-carbon of the β-alanine residue) is relatively unhindered, while the analogous torsional unit in **6** is more conformationally constrained because of the additional carbon substituent on the nitrogen. In particular, the C′N–$C_\beta C_\alpha$ torsional unit of **6** cannot be antiperiplanar, which would be antithetical to eight-membered-ring hydrogen-bond formation, while the C′N–$C_\beta C_\alpha$ torsional unit of **8** is likely to prefer the antiperiplanar arrangement. We have previously shown that such $A^{1,3}$-like interactions involving tertiary amides can have a substantial impact on the folding of small molecules.[17c,27] This factor may also be important in promoting nine-membered-ring hydrogen bonding in **7**, but it is clear from the behavior of **9** that the nine-membered-ring interaction is favorable even without the $A^{1,3}$-like contribution.

We have previously characterized the hydrogen-bond-mediated folding of members of the homologous diamide series **11–14** in organic solvents.[21] It is instructive to compare and contrast those earlier results with our present observations for several of the

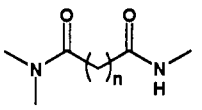

11, n = 1
12, n = 2
13, n = 3
14, n = 4

hydrogen-bonded ring sizes in methylene chloride. The six-membered-ring hydrogen-bonded form of **11** is nearly completely populated at all temperatures in liquid methylene chloride,[21] while the six-membered ring of **4** appears not to form to any extent in this temperature range. The eight-membered-ring hydrogen-bonded state of **13** is enthalpically preferred by only ca. 0.4 kcal/mol relative to the non-hydrogen-bonded state,[17c] while the eight-membered-ring hydrogen-bonded state of **6** is ca. 1.4 kcal/mol more favorable than the non-hydrogen-bonded state. In contrast to these differences for smaller ring sizes, the nine-membered-ring hydrogen-bonded states seem to be similarly favorable enthalpically for both **14** and **7** (by ca. 1.5 kcal/mol in each case). These comparisons highlight the fact that ring size itself is not the most important determinant of the thermodynamics of hydrogen-bonded ring closure. In each case, the folding process is promoted by formation of an amide-to-amide hydrogen bond, but folding is opposed by torsional strain and any other unfavorable interactions that develop as the molecule bends back upon itself. Therefore, the sequence of bond types (e.g., torsional preferences) in the segment linking the hydrogen-bond donor and acceptor sites is crucial, and different covalent bond sequences can lead to very different folding propensities for a given hydrogen-bonded ring size.

Benchmarks for Computational Methods. There is increasing interest in the use of computational methods to evaluate phenomena that are controlled by networks of noncovalent interactions (e.g., protein-folding pattern prediction and drug design).[28] Computational methods that are suitable for large molecules and molecular assemblies usually depend upon empirically derived parameters. Parametrization of covalent interaction terms, particularly for first-row elements, generally benefits from the availability of copious relevant experimental data.[29] Parametrization of *noncovalent* interaction terms, however, is more challenging, because of the paucity of relevant data. Our previous reports on hydrogen-bond-mediated folding of small amides in organic solvents have spawned computational studies that have shown some popular methods (AMBER[30] and AM[31]) to be deficient in their ability to evaluate the relative stabilities of alternative folding patterns. (McDonald and Still have recently demonstrated that AMBER*, a modified version of the original force field, is more successful at predicting hydrogen-bonding preferences in our systems.[32]) The behavior we have reported for diamides **4–9** provides additional benchmarks for the computational chemist interested in evaluating the ability of a given method to reproduce the folding behavior of flexible polar molecules in solution. Diamides **4** and **8**, which experience no intramolecular hydrogen bonding in methylene chloride, should be particularly useful in this context, because previous work has shown that empirical computational methods tend to overemphasize the conformation-directing roles of intramolecular hydrogen bonds.[6,30] Indeed, very recent MM2 studies of structures related to **8** suggest

(25) Arnett, E. M.; Mitchell, E. J.; Murty, T. S. S. R. *J. Am. Chem. Soc.* **1974**, *96*, 3875.
(26) (a) Johnson, F. *Chem. Rev.* **1968**, *68*, 375. (b) Berg, U.; Sanström, J. *Adv. Phys. Org. Chem.* **1989**, *25*, 1. (c) Hoffmann, R. W. *Angew. Chem., Int. Ed. Engl.* **1992**, *31*, 1124.
(27) Liang, G.-B.; Dado, G. P.; Gellman, S. H. *J. Am. Chem. Soc.* **1991**, *113*, 3994.
(28) For leading references, see: (a) Tidor, B.; Karplus, M. *Biochemistry* **1991**, *30*, 3217. (b) Kollman, P. A.; Merz, K. M. *Acc. Chem. Res.* **1990**, *23*, 246.
(29) Burkert, U.; Allinger, N. L. *Molecular Mechanics*; American Chemical Society Monograph No. 177; American Chemical Society: Washington, DC, 1982.
(30) Smith, D. A.; Vijayakumar, S. *Tetrahedron Lett.* **1991**, *32*, 3613, 3617. For a critical evaluation of these AMBER studies, see: Gellman, S. H.; Dado, G. P. *Tetrahedron Lett.* **1991**, *32*, 7737.
(31) Novoa, J. J.; Whangbo, M.-H. *J. Am. Chem. Soc.* **1991**, *113*, 9017. For a critical evaluation of this AM1 study, see ref 16.
(32) McDonald, D. Q.; Still, W. C. *Tetrahedron Lett.* **1992**, *33*, 7743, 7747.

that the lowest energy conformations of the isolated molecule do not contain an intramolecular hydrogen bond.[33]

Conclusion. We have postulated that the ability of polymers composed of α-amino acids to adopt compact and specific folding patterns results in part from the unfavorability of intramolecular hydrogen bonds between nearest neighbor amide groups in the polymer backbone. As a first step toward unnatural amide-based polymers that will adopt compact and specific folding patterns, we have evaluated the tendency for intramolecular hydrogen bond formation in derivatives of β-alanine and γ-amino butyric acid. Hydrogen bonds between neighboring amides appear to be favorable in the latter but not in the former. We are currently evaluating the folding properties of oligomeric β-peptides (i.e., molecules containing several β-amino acid residues).

Experimental Section

General Methods. All melting points are uncorrected. THF was freshly distilled from sodium benzophenone ketyl under N_2. Triethylamine was distilled from CaH_2 before use, and DMF was stored over 4-Å sieves. DMSO was distilled from CaH_2 and stored over 4-Å sieves. Reagents were used as obtained from commercial suppliers. For Boc removal, 4 N HCl in dioxane from Pierce Chemical Co. was used. Routine ^{1}H NMR spectra were obtained on a Bruker WP-200 spectrometer and are referenced to residual protonated NMR solvent in all cases. Routine ^{13}C NMR spectra were obtained on either a Bruker WP-270 or a Bruker AM-500 spectrometer and are referenced to the NMR solvent. High-resolution electron impact ionization mass spectroscopy was performed on a Kratos MS-80. Routine FT-IR spectra were recorded at room temperature on either a Nicolet 740 or a Mattson Polaris spectrometer. Column chromatography was carried out by using low N_2 pressure (typically 6 psi) with 230–400-mess silica gel 60 from EM Science. Columns eluted with low percentages of MeOH in $CHCl_3$ were slurry-packed after the slurry had been stirred with the eluant for from several hours to overnight. Fresh solvent was then passed through the column until changes in the gray hue of the silica had moved completely through the column bed. For columns eluted with EtOAc, the silica gel was dry-packed. Amides used for spectroscopic studies were estimated to be >95% pure on the basis of 500-MHz ^{1}H NMR spectra. Variable-temperature IR and ^{1}H NMR measurements were carried out as previously described.[21]

3-Bromopropanol Tetrahydropyranyl Ether. To a solution of 4.17 g (30 mmol) of 3-bromopropanol and 0.57 g (3 mmol) of *p*-toluenesulfonic acid monohydrate in 60 mL of dioxane was slowly added 8.2 mL (90 mmol) of 3,4-dihydro-2*H*-pyran.[34] After 45 min, the solution was neutralized to pH 7 with saturated aqueous $NaHCO_3$ and partitioned between 50 mL of H_2O and 150 mL of EtOAc. The layers were separated, and the aqueous layer was extracted with two 150-mL portions of EtOAc. The combined organic layers were dried over $MgSO_4$ and evaporated to a yellow oil. Purification by SiO_2 column chromatography eluting with 7.5% Et_2O in hexane gave the desired tetrahydropyranyl ether as a colorless liquid in 84% yield: ^{1}H NMR ($CDCl_3$) δ 4.58 (m, 1H, CH), 3.91–3.80 (m, 2H, OCH_2), 3.52 (t, J = 6.4 Hz, 2H, $BrCH_2$), 3.50–3.44 (m, 1H, OCH_2), 2.11 (p, J = 6.2 Hz, 2H, CH_2), 1.77–1.50 (m, 6H, 3 CH_2); IR (CCl_4) 2944 (CH), 2873 (CH), 1035 cm^{-1} (CO); EI MS m/e 221.0183, calcd for $C_8H_{14}O_2{}^{79}Br$ (M^+ – H) 221.0178; m/e 223.0158, calcd for $C_8H_{14}O_2{}^{81}Br$ (M^+ – H) 223.0158; calcd $^{79}Br/^{81}Br$ 1.02, found 1.05.

4-Chlorobutanol tetrahydropyranyl ether was prepared from 4-chlorobutanol by a procedure analogous to that for the preparation of 3-bromopropanol tetrahydropyranyl ether. The crude product was purified by SiO_2 column chromatography eluting with $CHCl_3$ to afford the desired compound in 58% yield as a colorless oil: ^{1}H NMR ($CDCl_3$) δ 4.56 (m, 1H, CH), 3.90–3.68 (m, 2H, OCH_2), 3.57 (t, J = 6.6 Hz, 2H, $ClCH_2$), 3.52–3.36 (m, 2H, OCH_2), 1.96–1.50 (m, 10H, 5 CH_2); IR (CCl_4) 2944 (CH), 2873 (CH), 1036 cm^{-1} (C–O); EI MS m/e 192.0919, calcd for $C_9H_{17}O_2{}^{35}Cl$ 192.0917; m/e 194.0860, calcd for $C_9H_{17}O_2{}^{37}Cl$ 194.0888; calcd $^{35}Cl/^{37}Cl$ 3.09, found 2.91.

***N*-(3-(Tetrahydropyranyloxy)propyl)valerolactam.** Tetrabutylammonium bromide (0.77 g, 2.4 mmol) was added to a slurry of 0.74 g (132 mmol) of pulvarized KOH in 10 mL of anhydrous THF. To this mixture was added dropwise a solution of 1.99 g (120 mmol) of valerolactam and 2.68 g (120 mmol) of 3-bromopropanol tetrahydropyranyl ether in 5 mL of THF, followed by an additional 5 mL of THF. After the reaction mixture was stirred under N_2 for 22 h at room temperature, solids were gravity filtered, and the filtrate was evaporated to a yellow liquid. Purification by SiO_2 column chromatography eluting with 3% MeOH in $CHCl_3$ afforded the desired compound as a colorless liquid in 61% yield: ^{1}H NMR ($CDCl_3$) δ 4.54 (m, 1H, CH), 3.9–3.7 (m, 2H, CH_2), 3.49–3.32 (m, 4H, 2 CH_2), 3.29 (m, 2H, NCH_2), 2.35 (m, 2H, $COCH_2$), 1.89–1.49 (m, 12H, 6 CH_2); IR (CCl_4) 2945 (CH), 2874 (CH), 1645 cm^{-1} (amide I); EI MS m/e 240.1593, calcd for $C_{13}H_{22}NO_3$ (M^+ – H) 240.1600.

***N*-(4-(Tetrahydropyranyloxy)butyl)valerolactam** was prepared from valerolactam and 4-chlorobutanol tetrahydropyranyl ether by an analogous procedure, except that the reaction mixture was refluxed under N_2 for 9 h. Purification by SiO_2 column chromatography eluting with 2% MeOH in $CHCl_3$ afforded the desired material as a yellow liquid (44% yield): ^{1}H NMR ($CDCl_3$) δ 4.56 (m, 1H, CH), 3.91–3.72 (m, 2H, CH_2), 3.54–3.41 (m, 4H, 2 CH_2), 3.38 (m, 2H, NCH_2), 2.36 (m, 2H, $COCH_2$), 1.89–1.53 (m, 14H, 7 CH_2); IR (CCl_4) 2945 (CH), 2869 (CH), 1646 cm^{-1} (amide I); EI MS m/e 255.1828, calcd for $C_{14}H_{25}NO_3$ 255.1834.

***N*-(3-Hydroxypropyl)valerolactam.** To a solution of 1.2 g (5 mmol) of lactam *N*-(3-(tetrahydropyranyloxy)propyl)valerolactam in 10 mL of MeOH was added 0.15 g of Amberlyst-15 ion-exchange resin.[35] After the reaction mixture was stirred for 6 h at 45 °C, the solids were removed by filtration and washed with several portions of MeOH. Evaporation of the filtrate afforded the desired material as a yellow oil in 88% crude yield. NMR and TLC (EtOAc) indicated the product to be quite clean: ^{1}H NMR ($CDCl_3$) δ 4.16 (t, J = 7.0 Hz, 1H, OH), 3.54–3.43 (m, 4H, NCH_2, OCH_2); 3.28–3.23 (m, 2H, NCH_2), 2.41–2.39 (m, 2H, OCH_2), 1.87–1.64 (m, 6H, 3 CH_2); IR (CCl_4) 3413 (OH), 2948 (CH), 2867 (CH), 1632 cm^{-1} (amide I); EI MS m/e 157.1103, calcd for $C_8H_{15}NO_2$ 157.1103.

***N*-(4-Hydroxybutyl)valerolactam** was prepared by deprotection of the corresponding tetrahydropyranyl ether in an analogous procedure. The crude product, isolated as a yellow liquid in 77% yield, was indicated by NMR and TLC (15% MeOH/$CHCl_3$) to be quite pure: ^{1}H NMR ($CDCl_3$) δ 3.65 (t, J = 6.0 Hz, 2H, OCH_2), 3.38 (t, J = 6.9 Hz, 2H, NCH_2), 3.30–3.24 (m, 2H, NCH_2), 2.72 (broad, 1H, OH), 2.38–2.35 (m, 2H, OCH_2), 1.84–1.46 (m, 8H, 4 CH_2); IR (CCl_4) 3419 (OH), 2934 (CH), 2865 (CH), 1644 cm^{-1} (amide I); EI MS m/e 171.1269, calcd for $C_9H_{17}NO_2$ 171.1259.

***N*-(3-Oxopropyl)valerolactam.** To a magnetically stirred solution of 0.7 mL (7.7 mmol) of oxalyl chloride in 14 mL of CH_2Cl_2 at –60 °C was added by syringe a solution of 1.16 mL (15 mmol) of dimethyl sulfoxide in 4 mL of CH_2Cl_2 under N_2.[36] After 2 min, 1.1 g (7 mmol) of crude alcohol dissolved in 6 mL of CH_2Cl_2 was added by syringe, and the resulting solution was stirred under N_2 at –60 °C for 15 min. To this solution was added 4.9 mL (35 mmol) of triethylamine. After being stirred at –60 °C for 5 min, the cloudy reaction mixture was allowed to warm to room temperature, and 25 mL of H_2O was then added, dissolving all solids. The aqueous and organic layers were separated, and the aqueous layer was extracted with two 25-mL portions of CH_2Cl_2. The combined organic layers were washed with two 75-mL portions of saturated aqueous $CuSO_4$ and 75 mL of brine, dried over $MgSO_4$, and evaporated to afford the crude desired aldehyde as a yellow liquid in 51% yield. This material was carried on without purification: ^{1}H NMR ($CDCl_3$) δ 9.79 (t, J = 1.5 Hz, 1H, CHO), 3.63 (t, J = 6.6 Hz, 2H, NCH_2), 3.36–3.30 (m, 2H, NCH_2), 2.56 (td, J = 6.5, 1.5 Hz, 2H, $COCH_2$), 2.37–2.31 (m, 2H, $COCH_2$), 1.79–1.74 (m, 4H, 2 CH_2); EI MS m/e 155.0941, calcd for $C_8H_{13}NO_2$ 155.0946.

***N*-(4-Oxobutyl)valerolactam** was prepared by Swern oxidation via an analogous procedure. The desired aldehyde was isolated as a yellow liquid in 84% crude yield and was carried on without purification: ^{1}H NMR ($CDCl_3$) δ 9.75 (broad t, 1H, CHO), 3.36 (t, J = 7.1 Hz, 2H, NCH_2), 3.29–3.23 (m, 2H, NCH_2), 2.48 (td, J = 7.0, 0.9 Hz, 2H, $COCH_2$), 2.36–2.31 (m, 2H, $COCH_2$), 1.85 (p, J = 7.1 Hz, 2H, CH_2), 1.80–1.75 (m, 4H, 2 CH_2); EI MS m/e 169.1105, calcd for $C_9H_{15}NO_2$ 169.1103.

***N*-(2-Carboxyethyl)valerolactam.** To a solution of 0.6 g (15 mmol) of sodium hydroxide in 5 mL of H_2O was added 1.25 g (7.35 mmol) of silver nitrate in 5 mL of H_2O, resulting in precipitation of brown solids.[37]

(33) Rao, S. N.; Balaji, V. N.; Ramnarayan, K. *Curr. Sci.* **1993**, *64*, 46.
(34) Van Boom, J. H.; Herschied, J. D. M. *Synthesis* **1973**, 169.
(35) Bongini, A.; Cardillo, G.; Ovena, R.; Sandri, S. *Synthesis* **1979**, 618.
(36) Swern, D.; Mancuo, A. J. *Synthesis* **1981**, 165.
(37) Campaigne, E.; SeSuer, W. M. *Organic Syntheses*; John Wiley & Sons, Inc.: New York, 1963; Collect. Vol. IV, p 919.
(38) For references on peptide protection, deprotection, and coupling chemistry, see: Bodanzski, M.; Bodanzski, A. *The Practice of Peptide Synthesis*; Springer-Verlag: Berlin, 1984.

The mixture was cooled to 0 °C, and 0.54 g (3.5 mmol) of *N*-(3-oxopropyl)-valerolactam was added. After the reaction mixture was stirred for 5 min at 0 °C, the solids were removed by suction filtration and washed with several portions of H_2O. The aqueous filtrate was washed with two 25-mL portions of EtOAc, acidified to pH <2 with concentrated HCl, and extracted with sixteen 25-mL portions of EtOAc. The combined organic layers were dried over $MgSO_4$ and evaporated to afford the desired carboxylic acid in 59% crude yield. NMR analysis indicated the product to be quite clean: ^{1}H NMR ($CDCl_3$) δ 8.53 (broad, 1H, COOH), 3.64 (t, J = 6.7 Hz, 2H, NCH_2), 3.40–3.34 (m, 2H, NCH_2), 2.68 (t, J = 6.6 Hz, 2H, $HOOCCH_2$), 2.46–2.40 (m, 2H, $COCH_2$), 1.88–1.80 (m, 4H, 2 CH_2); EI MS m/e 171.0904, calcd for $C_8H_{13}NO_3$ 171.0895.

***N*-(3-Carboxypropyl)valerolactam** was prepared by oxidation of *N*-(4-oxobutyl)valerolactam via an analogous procedure. The desired acid, isolated as a viscous orange syrup, was obtained in 98% crude yield and was carried on without purification: ^{1}H NMR ($CDCl_3$) δ 12.97 (s, 1H, COOH), 3.41 (t, J = 7.1 Hz, 2H, NCH_2), 3.31 (m, 2H, NCH_2), 2.49–2.46 (m, 2H, $COCH_2$), 2.32 (t, J = 7.1 Hz, 2H, $HOOCCH_2$), 1.90–1.56 (m, 6H, 3 CH_2); EI MS m/e 185.1049, calcd for $C_9H_{15}NO_3$ 185.1052.

Lactam 6. To a solution of 0.34 g (2 mmol) of *N*-(2-carboxyethyl)-valerolactam in 17 mL of DMF was added 0.345 g (3 mmol) of *N*-hydroxysuccinimide and 0.515 g (2.5 mmol) of dicyclohexylcarbodiimide; a white precipitate formed within 15 min.[37] After the mixture had been stirred under N_2 for 1 h, 0.41 g (6 mmol) of methylamine hydrochloride and 1 mL of triethylamine were added, and the slurry was stirred under N_2 for 20 h. The precipitate was then removed by gravity filtration. After concentration of the filtrate, the crude product was purified by SiO_2 column chromatography eluting with 3% MeOH in $CHCl_3$ to afford slightly impure lactam **6** in 70% crude yield. Further purification by stirring over Norrit-A decolorizing carbon in Et_2O and $CHCl_3$ afforded pure lactam in 54% yield as a nearly colorless viscous oil: ^{1}H NMR ($CDCl_3$) δ 6.81 (broad, 1H, NH), 3.61 (t, J = 6.6 Hz, 2H, NCH_2), 3.35–3.29 (m, 2H, NCH_2), 2.77 (d, J = 4.8 Hz, 3H, $NHCH_3$), 2.50 (t, J = 6.5 Hz, 2H, $COCH_2$), 2.35 (m, 2H, $COCH_2$), 1.81–1.74 (m, 4H, 2 CH_2); ^{13}C NMR ($CDCl_3$) δ 171.4, 170.3, 48.6, 44.1, 34.4, 32.1, 26.1, 23.1, 21.0; IR (0.001 M in CH_2Cl_2) 3455 (NH), 3295 (NH), 1672 (amide I), 1657 (amide I), 1627 cm^{-1} (amide I); EI MS m/e 184.1210, calcd for $C_9H_{16}N_2O_2$ 184.1212.

Lactam 7. To a solution of 0.326 g (1.75 mmol) of *N*-(3-carboxypropyl)valerolactam in 9 mL of THF were added 0.3 g (2.6 mmol) of *N*-hydroxysuccinimide and 0.45 (2.2 mmol) of dicyclohexylcarbodiimide; a white precipitate developed within 15 min. After being stirred at room temperature under N_2 for 2 h, the mixture was cooled to 0 °C in an ice bath and CH_3NH_2 gas was bubbled through for 10 min. After being stirred at 0 °C for 0.5 h, the reaction mixture was stirred under N_2 at room temperature for 8 h. The precipitate was then removed by gravity filtration, and the filtrate was concentrated to an orange syrup. Purification by SiO_2 column chromatography (2% MeOH in $CHCl_3$) and treatment with Norrit-A decolorizing carbon afforded the desired compound as a slightly yellow viscous oil in 18% yield: ^{1}H NMR ($CDCl_3$) δ 6.94 (broad, 1H, NH), 3.40 (t, J = 6.5 Hz, 2H, NCH_2), 3.30–3.24 (m, 2H, NCH_2), 2.79 (d, J = 4.8 Hz, 3H, $NHCH_3$), 2.37–2.31 (m, 2H, $COCH_2$), 2.16 (t, J = 5.9 Hz, 2H, $COCH_2$), 1.92–1.76 (m, 6H, 3 CH_2); ^{13}C NMR ($CDCl_3$) δ 173.2, 170.5, 47.6, 46.0, 33.2, 32.1, 26.1, 23.0, 21.0; IR (0.001 M in CH_2Cl_2) 3457 (NH), 3303 (NH), 1665 (amide I), 1622 cm^{-1} (amide I); EI MS m/e 198.1370, calcd for $C_{10}H_{18}N_2O_2$ 198.1368.

***N*-*tert*-Butyloxycarbonyl-β-alanine.** To a solution of 1.8 g (20 mmol) of β-alanine in 25 mL of H_2O and 50 mL of dioxane was added 5.55 g (40 mmol) of K_2CO_3. The solution was cooled to 0 °C in an ice bath, and 4.8 g (22 mmol) of di-*tert*-butyl dicarbonate was added. The reaction mixture was warmed to room temperature and stirred for 2.5 h. After concentration of the mixture by vacuum rotary evaporation, the residue was dissolved in 60 mL of H_2O and washed with two 100-mL portions of EtOAc. The aqueous layer was cooled to 0 °C and acidified to pH 3 with 80 mL of 1 N HCl. This mixture was extracted with five 100-mL portions of EtOAc. The combined organic layers were dried over $MgSO_4$, filtered, and evaporated to afford *N*-*tert*-butyloxycarbonyl-β-alanine as a white solid in 88% crude yield. This material was used without purification: mp 77.5–79 °C; ^{1}H NMR ($CDCl_3$) δ 9.5 (broad, 1H, COOH), 6.29 (broad, 1H, NH), 3.42–3.29 (m, 2H, $NHCH_2$), 2.58–2.46 (m, 2H, $COCH_2$), 1.45 (s, 9H, $C(CH_3)_3$); IR (CH_2Cl_2) 3450 (NH), 3340 (NH), 1714 (C=O), 1506 cm^{-1} (amide II); EI MS m/e 190.1094, calcd for $C_8H_{16}NO_4$ (M^+ + H) 190.1094.

***N*-*tert*-Butyloxycarbonyl-β-alanine *N'*,*N'*-dimethylamide** was prepared from *N*-*tert*-butyloxycarbonyl-β-alanine and dimethylamine in a procedure analogous to that for the preparation of lactam **6** from the corresponding acid. The crude product was purified by SiO_2 column chromatography eluting with EtOAc and then 5% MeOH in $CHCl_3$ to afford the desired amide as a colorless liquid in 78% yield: ^{1}H NMR ($CDCl_3$) δ 5.34 (broad, 1H, NH), 3.40 (q, J = 5.7 Hz, 2H, $NHCH_2$), 2.97 (s, 3H, NCH_3), 2.94 (s, 3H, NCH_3), 2.48 (t, J = 5.6 Hz, 2H, $COCH_2$), 1.41 (s, 9H, $C(CH_3)_3$; IR (CH_2Cl_2) 3449 (NH), 1706 (carbamate C=O), 1640 (amide I), 1500 cm^{-1} (amide II); EI MS m/e 216.1465, calcd for $C_{10}H_{20}N_2O_3$ 216.1474.

***N*-Acetyl-β-alanine *N'*,*N'*-dimethylamide (4)** was prepared from *N*-*tert*-butyloxycarbonyl-β-alanine *N'*,*N'*-dimethylamide in DMF by a procedure analogous to that for the preparation of diamide **8**. The crude product was purified by SiO_2 column chromatography eluting with 2–4% MeOH in $CHCl_3$ to afford 1.41 g of the desired material as a white solid in 41% yield: mp 49–51.5 °C; ^{1}H NMR ($CDCl_3$) δ 6.46 (broad, 1H, NH), 3.52 (q, J = 5.7 Hz, 2H, $NHCH_2$), 2.97 (s, 3H, NCH_3), 2.95 (s, 3H, NCH_3), 2.50 (t, J = 5.5 Hz, 2H, $COCH_2$), 1.93 (s, 3H, $COCH_3$); ^{13}C NMR ($CDCl_3$) δ 171.5, 169.9, 36.8, 35.0, 34.9, 32.8, 23.2; IR (CH_2Cl_2) 3440 (NH), 1667 (amide I), 1640 cm^{-1} (amide I); EI MS m/e 158.1051, calcd for $C_7H_{14}N_2O_2$ 158.1055.

***N*-*tert*-Butyloxycarbonyl-β-alanine *N'*-methylamide** was prepared from *N*-*tert*-butyloxycarbonyl-β-alanine and methylamine in a procedure analogous to that for the preparation of lactam **6** from the corresponding acid. The crude product was purified by SiO_2 column chromatography eluting with 2% MeOH in $CHCl_3$ to afford the desired amide as a white solid in 59% yield: mp 117.5–118.5 °C; ^{1}H NMR ($CDCl_3$) δ 5.95 (broad, 1H, NH), 5.23 (broad, 1H, Boc-NH), 3.40 (q, J = 6.1 Hz, 2H, $NHCH_2$), 2.81 (d, J = 4.8 Hz, 3H, $NHCH_3$), 2.40 (t, J = 6.1 Hz, 2H, $COCH_2$), 1.43 (s, 9H, $C(CH_3)_3$); IR (CH_2Cl_2) 3454 (NH), 3340 (NH), 1708 (carbamate C=O), 1672 (amide I), 1502 cm^{-1} (amide II); EI MS m/e 203.1396, calcd for $C_9H_{19}N_2O_3$ (M^+ + H) 203.1396.

***N*-(Acetyl-*tert*-butyloxycarbonyl)-β-alanine *N'*-Methylamide (8).** To 0.15 g (0.75 mmol) of *N*-*tert*-butyloxycarbonyl-β-alanine *N'*-methylamide was added 5 mL of 4 N HCl in dioxane. After being stirred under N_2 for 1 h, the solution was concentrated to a white solid and dried briefly on a vacuum line. The solid was dissolved in 5 mL of dioxane, and 0.42 mL (3 mmol) of triethylamine was added; a fine precipitate developed. The reaction mixture was cooled to 0 °C, and 0.14 mL (2 mmol) of acetyl chloride was slowly added under N_2. The resulting bright-yellow reaction mixture was allowed to warm to room temperature and stirred under N_2 for 19 h. The precipitate was then removed by gravity filtration. After concentration of the filtrate, the crude product was purified by SiO_2 column chromatography eluting with 6% MeOH in $CHCl_3$ to afford the desired amide as an off-white solid in 70% yield. This material was recrystallized from dichloroethane to afford a white crystalline solid in 45% yield: mp 146–146.5 °C; ^{1}H NMR ($CDCl_3$) δ 6.37 (broad, 1H, NH), 5.78 (broad, 1H, NH), 3.51 (q, J = 5.9 Hz, 2H, $NHCH_2$), 2.81 (d, J = 4.9 Hz, 3H, $NHCH_3$), 2.40 (t, J = 5.9 Hz, 2H, $COCH_2$), 1.96 (s, 3H, $COCH_3$); ^{13}C NMR ($CDCl_3$) δ 172.1, 170.3, 35.5, 35.4, 26.2, 23.3; IR (0.001 M in CH_2Cl_2) 3453 (NH), 1671 cm^{-1} (amide I); EI MS m/e 144.0908, calcd for $C_6H_{12}N_2O_2$ 144.0899.

***N*-*tert*-Butyloxycarbonyl-γ-amino butyric acid** was prepared from γ-aminobutyric acid in 98% crude yield as a viscous, colorless oil by a procedure analogous to that for the preparation of *N*-*tert*-butyloxycarbonyl-β-alanine. This material was carried on without purification: ^{1}H NMR ($CDCl_3$) δ 9.74 (broad, 1H, COOH), 4.80 (broad, 1H, NH), 3.16 (q, J = 6.2 Hz, 2H, NCH_2), 2.36 (t, J = 7.3 Hz, $COCH_2$), 1.79 (p, J = 7.0 Hz, 2H, CH_2), 1.41 (s, 9H, $C(CH_3)_3$); IR (CH_2Cl_2) 3450 (NH), 1711 (C=O), 1509 cm^{-1} (amide II); EI MS m/e 147.0533, calcd for $C_5H_9NO_4$: (M^+ – C_4H_8) 147.0532.

***N*-*tert*-Butyloxycarbonyl-γ-aminobutyric acid *N'*,*N'*-dimethylamide** was prepared from *N*-*tert*-butyloxycarbonyl-γ-aminobutyric acid and dimethylamine in a procedure analogous to that used for the preparation of lactam **6** from the corresponding acid. Purification by three silica flash columns (first column, 4% MeOH in $CHCl_3$; second column, EtOAc, followed by 3% MeOH in $CHCl_3$; third column, EtOAc) afforded the desired amide as a colorless, viscous oil in 76% yield: ^{1}H NMR ($CDCl_3$) δ 4.97 (broad, 1H, NH), 3.03 (q, J = 6.6 Hz, 2H, NCH_2), 2.92 (s, 3H, NCH_3), 2.86 (s, 3H, NCH_3), 2.28 (t, J = 7.2 Hz, 2H, $COCH_2$), 1.75 (p, J = 6.9 Hz, 2H, CH_2), 1.35 (s, 9H, $C(CH_3)_3$); IR (CH_2Cl_2) 3451 (NH), 3300 (NH), 1708 (carbamate C=O), 1640 (amide I), 1507 cm^{-1} (amide II); EI MS m/e 230.1635, calcd for $C_{11}H_{12}N_2O_3$ 230.1630.

***N*-Acetyl-γ-aminobutyric acid *N'*,*N'*-dimethylamide (5)** was prepared from *N*-*tert*-butyloxycarbonyl-γ-aminobutyric acid *N'*,*N'*-dimethylamide in procedure analogous to that used for the preparation of **4**. Purification by four silica flash columns (first and second columns, 5% MeOH in

$CHCl_3$; third and fourth columns, EtOAc, followed by 5% MeOH in $CHCl_3$) afforded the desired diamide as a colorless, viscous oil in 54% yield: ^1H NMR ($CDCl_3$) δ 6.49 (broad, 1H, NH), 3.26 (q, J = 6.2 Hz, 2H, $NHCH_2$), 2.99 (s, 3H, NCH_3), 2.94 (s, 3H, NCH_3), 2.38 (t, J = 6.6 Hz, 2H, $COCH_2$), 1.94 (s, 3H, $COCH_3$), 1.85 (p, J = 6.6 Hz, 2H, CH_2); ^{13}C NMR ($CDCl_3$) δ 172.5, 170.1, 39.3, 37.0, 35.2, 30.8, 24.1, 22.9; IR (0.001 M in CH_2Cl_2) 3446 (NH), 3323 (NH), 1670 (amide I), 1638 cm^{-1} (amide I); EI MS m/e 172.1214, calcd for $C_8H_{16}N_2O_2$ 172.1212.

***N*-*tert*-Butyloxycarbonyl-γ-aminobutyric acid *N'*-methylamide** was prepared from *N*-*tert*-butyloxycarbonyl-γ-aminobutyric acid in a procedure analogous to that for the preparation of lactam **6** from the corresponding acid. Purification by SiO_2 column chromatography eluting with 2% MeOH in $CHCl_3$ afforded the desired amide as a white solid in 76% yield: mp 120–121.5 °C; ^1H NMR ($CDCl_3$) δ 6.15 (broad, 1H, NH), 4.76 (broad, 1H, carbamate NH), 3.16 (q, J = 6.4 Hz, 2H, NCH_2), 2.81 (d, J = 4.8 Hz, 3H, $NHCH_3$), 2.21 (t, J = 6.9 Hz, 2H, $COCH_2$), 1.80 (p, J = 6.6 Hz, 2H, CH_2), 1.44 (s, 9H, $C(CH_3)_3$); IR (CH_2Cl_2) 3457 (NH), 3328 (NH), 1706 (Carbamate C=O), 1670 (amide I), 1507 cm^{-1} (amide II); EI MS m/e 160.0855, calcd for $C_6H_{11}N_2O_3$ ($M^+ - C_4H_9$) 160.0848.

***N*-Acetyl-γ-aminobutyric acid *N'*-methylamide (9)** was prepared from *N*-*tert*-butyloxycarbonyl-γ-aminobutyric acid *N'*-methylamide in a procedure analogous to that used for **8**. The crude product was purified by SiO_2 column chromatography eluting with 2–5% MeOH to afford **9** as a white solid in 63% yield: mp 97–99 °C; ^1H NMR ($CDCl_3$) δ 6.12 (broad, 2H, NH), 3.29 (q, J = 6.2 Hz, 2H, $NHCH_2$), 2.81 (d, J = 4.8 Hz, 3H, $NHCH_3$), 2.23 (t, J = 6.6 Hz, 2H, $COCH_2$), 1.98 (s, 3H, $COCH_3$), 1.83 (p, J = 6.5 Hz, 2H, CH_2); ^{13}C NMR ($CDCl_3$) δ 173.5, 170.8, 39.1, 33.7, 26.2, 25.5, 23.2; IR (0.001 M in CH_2Cl_2) 3454 (NH), 3316 (NH), 1670 cm^{-1} (amide I); EI MS m/e 158.1041, calcd for $C_7H_{14}N_2O_2$ 158.1041.

Acknowledgment. This work was supported by the National Science Foundation (Grant CHE-9224561). G.P.D. is the recipient of a National Research Service Award (T32GM08923) from the National Institute of General Medical Sciences and a Dean's Fellowship from the University of Wisconsin—Madison. S.H.G. is a fellow of the Alfred P. Sloan Foundation. The FT-IR spectrometer was purchased with funds provided by the Office of Naval Research.